A&A 555, A116 (2013)
DOI: 10.1051/0004-6361/201321323

Astronomy & Astrophysics

Broad-band spectroscopy of the ongoing large eruption of the luminous blue variable R71⋆,⋆⋆,⋆⋆⋆

A. Mehner[1], D. Baade[2], T. Rivinius[1], D. J. Lennon[3], C. Martayan[1], O. Stahl[4], and S. Štefl[5]

[1] ESO – European Organisation for Astronomical Research in the Southern Hemisphere, Alonso de Cordova 3107, Vitacura, Santiago de Chile, Chile
e-mail: amehner@eso.org
[2] ESO – European Organisation for Astronomical Research in the Southern Hemisphere, Karl-Schwarzschild-Straße 2, 85748 Garching, Germany
[3] ESAC – European Space Astronomy Centre, Camino bajo del Castillo, Urbanizacion Villafranca del Castillo, Villanueva de la Cañada, 28692 Madrid, Spain
[4] Zentrum für Astronomie der Universität Heidelberg, Landessternwarte, Königstuhl 12, 69117 Heidelberg, Germany
[5] ESO/ALMA – The European Organisation for Astronomical Research in the Southern Hemisphere/The Atacama Large Millimeter/Submillimeter Array, Alonso de Cordova 3107, Vitacura, Santiago de Chile, Chile

Received 19 February 2013 / Accepted 26 May 2013

ABSTRACT

Aims. The luminous blue variable (LBV) R71 is currently undergoing an eruption, which differs photometrically and spectroscopically from its last outburst in the 1970s. Valuable information on the physics of LBV eruptions can be gained by analyzing the spectral evolution during this eruption and by comparing R71's present appearance to its previous outburst and its quiescent state.
Methods. An ongoing monitoring program with VLT/X-shooter will secure key spectral data ranging from visual to near-infrared wavelengths. Here we present the first spectra obtained in 2012 and compare them to archival VLT/UVES and MPG/ESO-2.2 m/FEROS spectra from 2002 to 2011. The discussed data include pre-eruption spectra in 2002 and 2005, a spectrum of the transitionary phase between quiescent and eruptive state in 2007, and spectra of the eruption in 2011–2012. Information on R71's 1970s outburst is taken from the literature.
Results. The 2011–2012 spectra are dominated by strong neutral and singly ionized metal absorption lines likely formed in a large "pseudo-photosphere". We find an unusually low apparent temperature of R71 of only $T_{\rm eff,2012} \sim 6\,650$ K; the star resembles a late F supergiant. R71's visual lightcurve had a maximum in 2012 with $m_{\rm V,2012} \sim 8.7$ mag. Given the uncertainty in the extinction toward R71, this corresponds to a bolometric luminosity of $M_{\rm bol,2012} \sim -9.8$ mag to -10.3 mag. R71's 2011–2012 spectra do not show H I and Fe II P Cyg profiles, which were present during its last outburst in the 1970s and which are normally observed during LBV outbursts. Low-excitation forbidden emission lines and Fe I P Cyg-like profiles from a slowly expanding nebula became apparent in late 2012. These lines originate likely in the rarefied region above the pseudo-photosphere up to 13 AU from the star.
Conclusions. The rise in R71's visual magnitude and the low apparent temperature of its pseudo-photosphere during the current eruption are unprecedented for this star. R71 most likely increased its bolometric luminosity by $\Delta M_{\rm bol} = 0.4$–1.3 mag compared to its quiescent state. The very low temperature of its pseudo-photosphere implies a very high-mass loss rate on the order of $\dot{M}_{\rm R71,2012} \sim 5 \times 10^{-4}\ M_\odot\ {\rm yr}^{-1}$ compared to $\dot{M}_{\rm quiescence} \sim 3 \times 10^{-7}\ M_\odot\ {\rm yr}^{-1}$. The apparent radius increased by a factor of 5 to about 500 $R_\odot$. No fast-moving material indicative of an explosion is observed. The changes in R71's photometry and spectrum are thus likely consequences of a tremendously increased wind density, which led to the formation of a pseudo-photosphere.

Key words. stars: variables: S Doradus – stars: winds, outflows – stars: individual: R71 – stars: massive

1. Introduction

The luminous blue variable (LBV) R71 (=HD 269006) in the Large Magellanic Cloud (LMC) is currently undergoing an eruption that started in 2005 (Gamen et al. 2009). In 2012 the star had reached unprecedented visual brightness, accompanied by remarkable variations in its optical spectrum (Gamen et al. 2012). R71's current eruption is characterized by more extreme parameters than its outburst in the 1970s and may provide us with important insights into the LBV phenomenon.

LBVs, also known as S Doradus variables, are evolved massive stars that exhibit a type of instability which is not yet understood (Conti 1984, 1997; Humphreys & Davidson 1994; Nota & Lamers 1997, and references therein). They represent a brief but critical phase in massive star evolution because several solar masses can be expelled during this stage. LBVs are generally considered to be stars in transition to the WR stage (e.g., Maeder 1983; Humphreys & Davidson 1994; Langer et al. 1994) but see below. The LBV phenomenon extends to luminosities as low as $\log(L/L_\odot) \sim 5.4$, corresponding to stars with initial masses of ~25 $M_\odot$. LBVs experience outbursts with enhanced mass loss during which they appear to make transitions in the Hertzsprung-Russell (HR) diagram

⋆ Based on observations collected at ESO's Very Large Telescope under Prog-IDs: 69.D-0390(D) and 289.D-5040(A) and at the MPG/ESO 2.2-m Telescope under Prog-IDs: 076.D-0609(A), 078.D-0790(B), 086.D-0997(A), and 087.D-0946(A).
⋆⋆ This work was co-funded under the Marie Curie Actions of the European Commission (FP7-COFUND).
⋆⋆⋆ Table 1 is available in electronic form at http://www.aanda.org

from their quiescent hot state ($T_{\rm eff} \sim 20\,000$–$30\,000$ K) to lower temperatures ($T_{\rm eff} \sim 8000$ K). Their instability could be responsible for the empirically found upper luminosity boundary (also known as Humphreys-Davidson limit) above and to the right of which no supergiants are found (Humphreys & Davidson 1979, 1984). The lowest luminosity LBVs likely have a short red supergiant (RSG) phase prior to becoming LBVs.

Most of the fundamental questions about the physical cause of the LBV instability are still unsolved and they may fall into different categories, i.e., classical LBV outbursts and giant eruptions. Outbursts with visual magnitude variations of 1–2 mag and constant bolometric luminosity are commonly referred to as classical LBV outbursts. During giant eruptions the visual magnitude increases by more than 2 mag and the bolometric luminosity likely increases. Historical examples of giant eruptions are P Cygni in the 17th century (e.g., de Groot 1988; Lamers & de Groot 1992), η Car in the 1840s (see the reviews by Davidson & Humphreys 1997, 2012 and references therein), V12 in NGC 2403 in the 1950s (e.g., Tammann & Sandage 1968; Smith et al. 2001), and SN1961V in NGC 1058 (e.g., Goodrich et al. 1989; Van Dyk & Matheson 2012; cf. Kochanek et al. 2011). The most promising explanation for the LBV instability mechanism involve radiation pressure instabilities, but also turbulent pressure instabilities, vibrations and dynamical instabilities, and binarity cannot be entirely ruled out (Humphreys & Davidson 1994, and references therein). It is unknown what the relative roles of classical LBV outbursts and giant eruptions are and which of the two events are more important in terms of total mass lost. It is also not established if giant eruptions result from unusual circumstances and due to a different instability mechanism or if they are only extreme cases of classical LBV outbursts.

Recent observational and theoretical works suggests that some LBVs can be the immediate progenitors of supernovae (SNe). Some core-collapse SNe may be boosted to very high luminosity when the ejecta shock circumstellar matter expelled during a previous LBV outburst and kinetic energy is converted to radiative energy (Smith et al. 2007, 2008)[1]. LBV-like eruptions immediately prior to SN explosions have been observed in a few cases; e.g., SN2005gl (Gal-Yam et al. 2007; Gal-Yam & Leonard 2009). Groh et al. (2013) found using stellar evolutionary models that single rotating stars with initial mass in the range of 20–25 $M_\odot$ have spectra similar to LBVs before exploding as SNe. This result sets the theoretical ground for low-luminosity LBVs, such as possibly R71 (but see Sect. 4), to be the endpoints of stellar evolution.

Important clues toward an understanding of the LBV phenomenon can be gained from their variabilities that occur on different magnitude and timescales (Humphreys & Davidson 1994, and references therein). R71 is excellent for a case study. It has been well-observed over the last decades and its location in the LMC is fortunate because its distance and reddening are well constrained. During its quiescent phase R71 has a hot supergiant spectrum with strong H I, He I, Fe II, and [Fe II] lines and P Cyg profiles. It was classified as a B2.5 Ieq star with $m_{\rm V} \sim 10.9$ mag (Feast et al. 1960). It has a typical supergiant mass loss rate of $\sim 3 \times 10^{-7}\ M_\odot\ {\rm yr}^{-1}$ (Wolf et al. 1981). The star shows microvariations of $\Delta m_{\rm V} \sim 0.1$ mag on timescales of 14–100 days attributed to large turbulent elements and dynamical instabilities in the photosphere or to pulsations (van Genderen et al. 1985, 1988, 1997; Lamers et al. 1998). R71 had a classical LBV outburst in 1970–1977 when it reached $m_{\rm V} \sim 9.9$ mag (Thackeray 1974; Wolf 1975; van Genderen 1979; Wolf et al. 1981; van Genderen 1982). During the outburst its mass loss rate increased by a factor of about 100 to $\sim 5 \times 10^{-5}\ M_\odot\ {\rm yr}^{-1}$ (Wolf et al. 1981, cf. Vink & de Koter 2002, who found that R71's mass loss rate increased only by a factor of 3–5).

R71's current eruption started in 2005. In 2012 the star had reached an unprecedented visual magnitude of $m_{\rm V} \sim 8.7$ mag and is currently the visually brightest star in the LMC[2]. At the end of 2012 a decline in R71's visual lightcurve commenced while the R-band lightcurve stayed bright (AAVSO). Gamen et al. (2009, 2012) found that the spectrum in 2008 February resembled an early-A supergiant, in 2009 August an extreme early-F hypergiant, and in 2012 that of an early-G supergiant.

In this paper we discuss R71's current eruption in relation to its previous outburst in the 1970s and to its quiescent state. Because of the rarity of LBV outbursts and their potential importance in massive star evolution this large-amplitude event calls for special attention. In Sect. 2 we describe the observations. In Sect. 3 we analyze the changes of selected spectral features in detail. In Sect. 4 we discuss the results and consider R71's classification as an underluminous or classical LBV. In Sect. 5 we summarize our conclusions.

2. Observations and data analysis

In 2012 August, September, and November we obtained the first X-shooter spectra of R71 of a long-term monitoring program at the Very Large Telescope (VLT). X-shooter is a medium-resolution echelle spectrograph that simultaneously observes with 3 arms covering the wavelength region from 3000–24 800 Å (Vernet et al. 2011). Spectra were obtained with the narrowest available slits of 0.″5 in the UVB arm, 0.″4 in the VIS arm, and 0.″4 in the near-infrared arm yielding spectral resolving powers of $R \sim 9000$–$17\,000$. In addition, spectra were obtained with the 5″ slits in all 3 arms to achieve an absolute flux calibration but also to investigate the spectral energy distribution.

We retrieved archival spectra of R71 obtained with VLT/UVES in 2002 and with MPG/ESO-2.2 m/FEROS in 2005, 2007, and 2011. The UVES spectra in 2002 were obtained during R71's quiescent state. They cover the wavelength region from 3000–6800 Å with spectral resolving power of $R \sim 40\,000$. The FEROS spectra cover the wavelength region from 3500–9200 Å with spectral resolving power of $R \sim 48\,000$ and were obtained throughout the current outburst starting at its onset in 2005.

A journal of observations is listed in Table 1. Each data set was reduced with the corresponding ESO pipeline (X-shooter pipeline version 1.5.0, UVES pipeline version 5.0.17, FEROS pipeline version 1.60). The spectra were corrected for the instrument response and atmospheric extinction but not for interstellar extinction and telluric lines. Figure 1 shows R71's visual lightcurve from 2000 November using data from the ASAS and from the AAVSO. The epochs of the here discussed spectra are indicated.

We used the 2002 UVES spectra to determine R71's systemic velocity. During the quiescent state the permitted lines show P Cyg profiles and we therefore used the [Fe II] emission lines at $\lambda\lambda$4287, 4414, 4416, 4452, 4458, 4489, 4728, 4890 Å, which originate in the outer stellar wind. We found

[1] See Quataert & Shiode (2012) for an alternative explanation.

[2] See Fig. 1 for R71's visual lightcurve since 2000 November using data from the All Sky Automated Survey (ASAS; Pojmanski 1997) and from the American Association of Variable Star Observers (AAVSO; http://www.aavso.org); cf. with Feast et al. (1960).

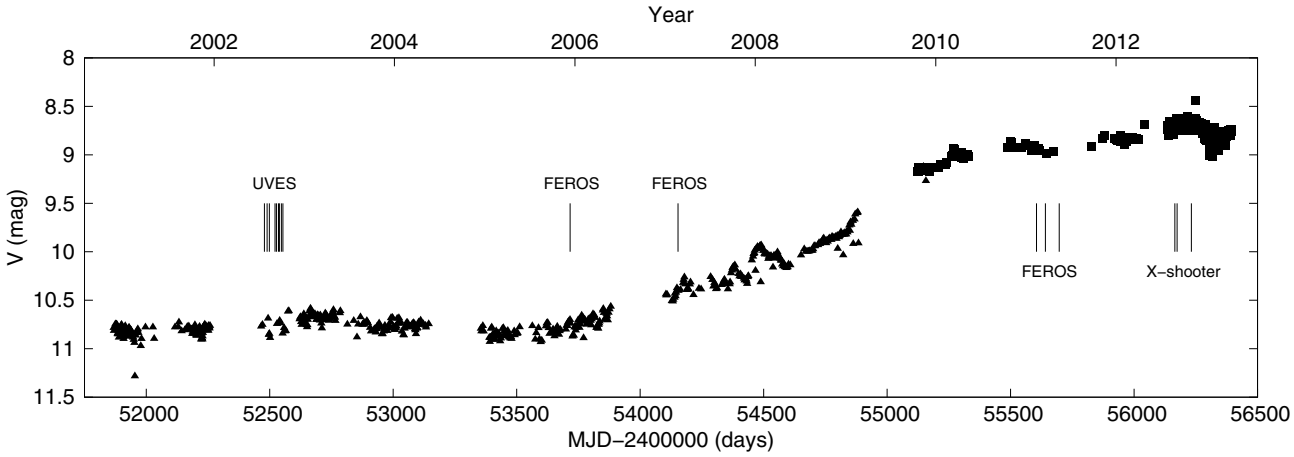

Fig. 1. R71's visual lightcurve. The triangles are data points from the ASAS and filled squares are from the AAVSO. Marks show when the spectra discussed in this paper were obtained. R71 brightened by more than 2 mag since 2005.

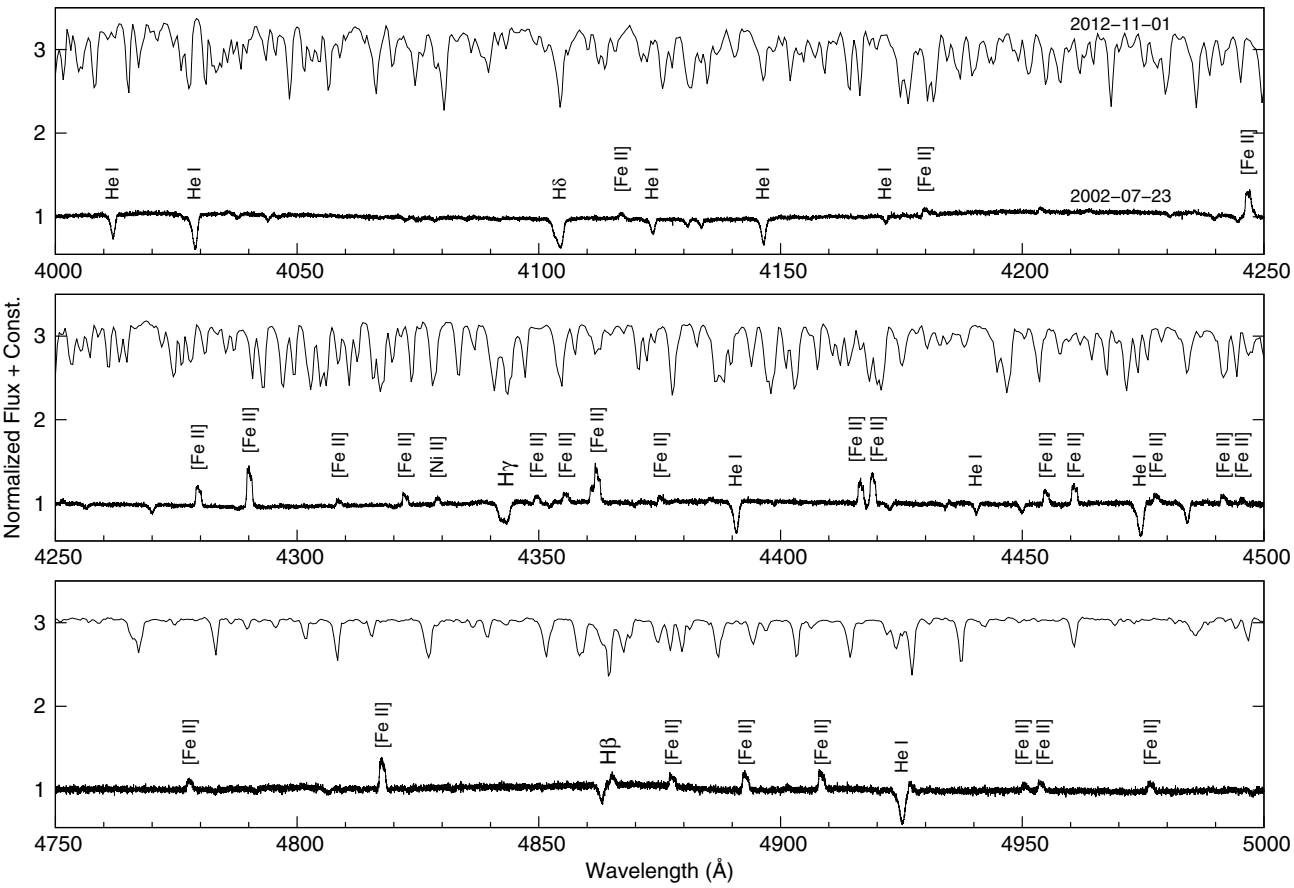

Fig. 2. Spectral variations between R71's quiescent state in 2002 July (*bottom* spectrum) and its eruptive state in 2012 November (*top* spectrum). The 2002 UVES spectrum shows strong [Fe II] emission. Hβ has a P Cyg profile, while higher Balmer lines and He I lines appear only in absorption. The 2012 X-shooter spectrum is dominated by strong metal absorption lines. (The continuum is normalized to unity. The wavelength region $\lambda\lambda$4500–4750 Å is not displayed because of a gap in wavelength between the UVES blue and red settings.)

$v_{\rm sys}$ = 192 ± 3 km s^{-1}, in good agreement with the literature values $v_{\rm sys}$ = 195 km s^{-1} (Thackeray 1974) and $v_{\rm sys}$ = 193 km s^{-1} (Wolf et al. 1981), which were also determined from [Fe II] lines. All radial velocities stated below are relative to the systemic velocity.

3. Results

The 2012 X-shooter spectra confirm the dramatic spectral changes reported in Gamen et al. (2012). However, the peak visual magnitude appears to have been lower (Fig. 1) as stated by Gamen et al. and we do not confirm that R71 currently resembles an early G-supergiant. Figure 2 compares a UVES spectrum obtained in 2002 July with an X-shooter spectrum obtained in 2012 November. Most emission lines have disappeared and the spectrum is dominated by strong neutral and singly ionized metal absorption lines (e.g., Fe I, Fe II, Si I, Si II, S I, N I, and O I) indicative of a cold dense pseudo-photosphere, which develops during an LBV outburst (Leitherer et al. 1985; Appenzeller 1986; Davidson 1987).

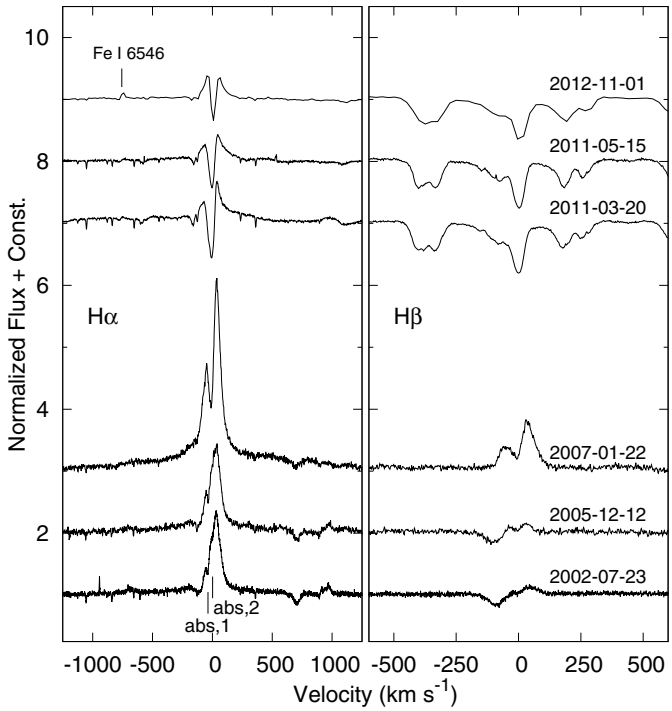

Fig. 3. Hα and Hβ in R71 from 2002–2012. The Hα P Cyg profile changed to an inverse double-peaked symmetric profile during the eruptive state. The absorption component close to system velocity now dominates the profile. Hβ behaves similarly to Hα. In the latest spectrum from 2012 November, the Fe I λ6546 emission line becomes apparent toward the blue of Hα. The strong absorption features to the red and blue of Hβ in 2011–2012 are blends of Fe I, Ni I, Ti I, Ti II absorption lines. (The continuum is normalized to unity, velocities are in R71's restframe.)

We analyzed several spectral features between 2002–2012. The UVES spectra in 2002 were obtained during the maximum of a microvariation ($m_V \sim 10.7$ mag compared to $m_V \sim 10.9$ mag in quiescence), see Fig. 1. Small variations in the line profiles occur during 2002 but the spectra nevertheless closely resemble R71's appearance in quiescent phase[3]. At the time the 2005 FEROS spectrum was obtained, the current eruption had already commenced ($m_V \sim 10.7$ mag). The 2002 July and 2005 December spectra show no major differences. The 2007 FEROS spectrum appears to be a snapshot of the transitionary phase between the quiescent and the eruptive state with $m_V \sim 10.3$ mag. The 2011 FEROS and 2012 X-shooter spectra show R71 in eruption when the visual magnitude reached up to $m_V \sim 8.7$ mag (cf. Gamen et al. 2012 who found a maximum brightness of $m_V \sim 8.3$ mag, which most likely was based on a single outlying data point).

3.1. Hydrogen lines

Figure 3 shows a time series of Hα and Hβ from 2002–2012. Hα changed from a P Cyg profile with broad emission wings extending up to $v_{em} \sim \pm 850$ km s^{-1} in 2002–2005 to a prominent double-peaked symmetric profile in 2011/2012. The maximum depth of the P Cyg absorption in 2002 July is at $v_{abs} = -118 \pm 12$ km s^{-1} and the blue edge is at $v_{edge} = -186 \pm 5$ km s^{-1}. We use the blue edge of the Hα P Cyg absorption as a proxy for the terminal velocity but since the absorption is not well-defined and filled in with extra emission this measurement gives only a lower limit. The profile shows two additional absorption features at $v_{abs,1} = -37 \pm 2$ km s^{-1} and at $v_{abs,2} = 2 \pm 6$ km s^{-1}. The former may be due to an expanding shell, while the latter originates most likely from the photosphere. In spectra obtained between 2002 August and October we find $v_{edge} = -131 \pm 20$ km s^{-1}. In 2007 extra emission compared to the continuum is observed indicating an increased mass loss rate. The P Cyg absorption has disappeared as has the absorption component at $v_{abs,1} \sim -37$ km s^{-1}. The weak absorption component at system velocity strengthened, most likely due to the formation of a cooler pseudo-photosphere. In 2011/2012 this absorption component dominates the Hα profile. It has a full width at half maximum (FWHM) of 44 ± 1 km s^{-1}. There was no indication of this absorption component during the previous outburst but this absorption feature was first observed in the 1990s. Weak broad Hα emission is still present and a weak absorption component can be observed with a blue edge at $v_{edge} = -199 \pm 9$ km s^{-1}.

We found comparable values for the blue edge of the Hα absorption during quiescence and eruption. However, because the Hα absorption depends on the density and ionization structure of the wind, and the star is currently hidden beneath a pseudo-photosphere, we cannot state for certain whether the wind velocity stayed unchanged during the current outburst. Our values of $v_{edge} \sim -131$ km s^{-1} to -199 km s^{-1} are comparable to the value $v_{edge} = -158$ km s^{-1} in 1984 found by Stahl & Wolf (1986). Wolf et al. (1981) found a maximum outflow velocity of $\sim$127 km s^{-1} in UV Fe II lines.

Hβ behaves similarly to Hα but does not show prominent line emission in 2011/2012. Higher Balmer lines are always in absorption. Paschen and Bracket lines (Brγ and higher), which were likely in emission during quiescent state, are in absorption in 2012. The absence of hydrogen emission (apart from Hα emission) indicates that R71's pseudo-photosphere is much cooler and denser during the current eruption than during its 1970s outburst when Hα to Hδ showed strong P Cyg profiles (Wolf et al. 1981).

3.2. Helium lines

Optical He I absorption at system velocity in pre-eruption spectra have disappeared in 2011/2012. During the 1970s outburst the spectrum showed He I absorption (Thackeray 1974), again indicating lower temperatures during the current eruption. We find an absorption feature at the near-infrared He I λ10830 line but not at He I λ17002. Because no near-infrared spectra during the quiescent state are available to us we cannot conclusively identify the absorption feature in the concerning wavelength region as He I λ10830. Likely no He I absorption and emission lines are present at the current time.

3.3. Ca II lines

Figure 4 compares Ca II lines in 2005 and in 2012. These lines provide information on the (changing) conditions of the pseudo-photosphere and the circumstellar material. Ca II has a low ionization potential and the broad and very deep Ca II H and K absorption lines observed in 2011 and 2012 are

[3] No significant line variations hinting at a potential companion is observed during the 3 months of UVES coverage. Comparison of the UVES spectra to the FEROS and X-shooter spectra with respect to line variations due to binarity is inhibited because of the spectral changes inflicted by the eruption.

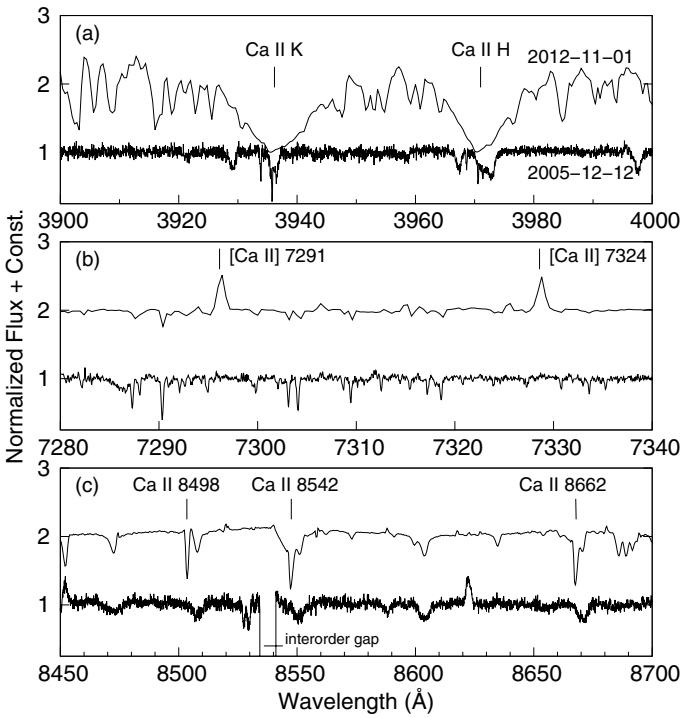

Fig. 4. Ca II lines in 2005 (bottom: FEROS spectrum) and 2012 (top: X-shooter spectrum); **a)** the Ca II H and K lines show very broad and deep absorption; **b)** the [Ca II] $\lambda\lambda$7291, 7324 lines are in emission; and **c)** the Ca II near-infrared lines at $\lambda\lambda$8498, 8542, 8662 Å are in absorption. The Paschen lines $\lambda\lambda$8502, 8545, 8665 Å can be seen in absorption just to the right of the Ca II triplet lines. (The continuum is normalized to unity.)

therefore an indicator of the low temperatures in R71's pseudo-photosphere. The forbidden [Ca II] $\lambda\lambda$7291, 7324 lines are in emission and the near-infrared triplet Ca II $\lambda\lambda$8498, 8542, 8662 is in absorption. The Ca II near-infrared triplet lines are usually observed in emission in warm hypergiants. They are formed by radiative de-excitation from the upper level of the Ca II H and K absorption, which leaves the Ca^+ ions in the upper level for the [Ca II] $\lambda\lambda$7291, 7324 lines[4]. We investigated the line variations in our 2012 spectra in order to explain the puzzling combination of Ca II near-infrared triplet absorption and [Ca II] $\lambda\lambda$7291, 7324 emission observed in R71. We find that the Ca II near-infrared triplet lines show the same residuals as the Hα emission, while pure photospheric lines vary little. The Ca II triplet is likely dominated by absorption but filled in by an emission component from the circumstellar material that may be sufficient to populate the upper level of the [Ca II] $\lambda\lambda$7291, 7324 lines[5].

3.4. Other metal lines

Other spectral lines confirm the very low temperature of R71's pseudo-photosphere. The optical to near-infrared spectrum in 2012 is dominated by strong neutral and singly ionized metal absorption lines (e.g., Fe I, Fe II, Mg II, Si I, Si II, S I, N I, and O I). In the previous outburst almost all lines (in particular the Balmer lines, Fe II, and Ti II) showed classical P Cyg profiles with a deep absorption component (Wolf et al. 1981), which is not the case for the current eruption. [Fe II] emission lines have disappeared. Mg II λ4481 absorption, indicative of low temperatures, is strong. The Na I $\lambda\lambda$5890, 5896 lines show three absorption components: 1.) the Galactic interstellar absorption with $v = -177 \pm 1$ km s^{-1} relative to R71, 2.) an absorption component with $v = 13 \pm 1$ km s^{-1}, which likely is the interstellar LMC feature, and 3.) a component with $v = -29 \pm 1$ km s^{-1}, which is conceivably formed in the cool pseudo-photosphere and the circumstellar material based on its line strength variations. The velocity of this component stayed constant compared to pre-outburst, but the line became stronger.

Between 2012 August and November Fe I emission lines appeared redwards of their absorption components (producing a P Cyg-like profile). In Fig. 3, e.g., the Fe I λ6546 line can be seen in the latest spectrum. According to Kovtyukh et al. (2011) the observed equivalent width ratio of Fe I λ6430 to Fe I λ6421 of ~2, i.e., different from about unity, would indicate a nonthermal excitation mechanism. Other emission lines characteristic of a very low-excitation "nebula" (excitation energy on the order of 4 eV and less) appeared and became stronger. We tentatively identify narrow emission from, e.g., [O I] $\lambda\lambda$6300, 6364, 6392, [Ni I] λ7394, and [S I] $\lambda\lambda$7725,10821. These lines indicate the presence of a neutral nebula, likely ejected during the current eruption and possibly the rarefied region above the pseudo-photosphere. The Fe I emission lines, which appeared in late 2012, may originate from the same region. Classical nebular lines from an ionized nebula such as [N II] $\lambda\lambda$6548, 6583, which were observed in R71's spectrum in 1984 (Stahl & Wolf 1986), are not present. The expansion velocity of the nebula is on the order of a few km s^{-1} and thus small compared to the stellar wind velocity. The eruption started about 6 years ago and, if we assume an expansion velocity of $v_{\rm eruption} \sim 10$ km s^{-1}, the ejected material is now reaching a distance of about 13 AU or 3000 $R_\odot$ from the star. At a distance of the LMC, this corresponds to about 0.3 mas. Even though R71 showed nebular lines and evidence of a dust shell before the current eruption, Weis (2003) found no extended optical nebula in the HST/WFPC2 image of R71 obtained in 1998. If R71 formed an LBV nebula during its 1970s outburst, it is either extremely faint or very small (<0.5″). The observed weak emission lines may also originate from this formerly ejected material.

Photometrically and spectroscopically, R71's current eruption is very different compared to its previous outburst. Its visual lightcurve reached a peak magnitude in 2012 that was about 1 mag brighter than during the 1970s outburst and R71's current spectrum implies a much cooler pseudo-photosphere.

4. Discussion

R71 was well-observed over the last decades covering its quiescent phases and its 1970–1977 classical LBV outburst. This gives us a unique opportunity to compare the current eruption to its previous behavior. Table 2 gives an overview of R71's parameters found for its quiescent state and its 1970s outburst by different authors, and parameters estimated in this paper for its current eruption.

There is ambiguity in the literature regarding the classification of R71 as a classical LBV (Lennon et al. 1993) or as a less luminous LBV (Wolf et al. 1981). Reasons are the uncertainty in the extinction toward R71 and the bolometric correction, see Table 2. To interpret R71's behavior it is important to know to which of the two groups it belongs because they differ in mass

[4] Alternatively, Prieto et al. (2009) and Smith et al. (2009) have suggested that the [Ca II] $\lambda\lambda$7291,7324 emission lines may be due to dust destruction. However, it is unclear what would cause the destruction of dust during this eruption.

[5] The Ca II triplet was seen in emission before 2012 but then declined (Gamen et al. 2012).

Table 2. Parameters of R71.

State	Source	m_V (mag)	DM_{LMC} (mag)	A_V^1 (mag)	T_{eff} (K)	BC (mag)	log $(L/L_\odot)^2$	M_{bol}^2 (mag)
Quiescence	Wolf et al. (1981)	10.88	18.50	0.15	13 600	–0.76	5.30	–8.53
	van Genderen (1982)	10.89	18.60	0.15	14 000	–0.95	5.37	–8.71
	van Genderen (1988)	10.87	18.60	0.37	14 700	–1.10	5.53	–9.10
	Lennon et al. (1993)	10.88	18.45	0.63	17 250	–1.69	5.86	–9.94
Outburst 1970–1977	van Genderen (1982)	9.79	18.60	0.15	11 000	–0.38	5.58	–9.24
	van Genderen (1988)	9.77	18.60	0.37	8150	–0.10	5.57	–9.20
Outburst 2012	this paper	8.7[3]	18.50[4]	0.15[5]	6650	0.11	5.82	-9.84
		8.7[3]	18.50[4]	0.37[6]	6650	0.11	5.91	–10.06
		8.7[3]	18.50[4]	0.63[7]	6650	0.11	6.02	–10.32

Notes. [(1)] In the cases were only $E(B–V)$ was given in the literature, we adopted the standard extinction law with $R_V = A_V/E(B–V) = 3.1$ (Howarth 1983). [(2)] Values were (re-)calculated using $DM_{LMC} = 18.5$ mag and may therefore deviate from the cited literature. [(3)] Determined from the AAVSO, but see Gamen et al. (2012). [(4)] E.g., Freedman et al. (2001); Pietrzyński et al. (2013). [(5)] Wolf et al. (1981). [(6)] van Genderen et al. (1988). [(7)] Lennon et al. (1993).

and evolutionary path (Humphreys & Davidson 1994). Classical LBVs have $M_{bol} < -9.6$ mag and have very likely not been RSGs. Less luminous LBVs have $M_{bol} = -8$ mag to -9 mag, lower temperatures, smaller amplitudes of their outbursts, and lower mass loss rates. They have probably been RSGs.

Support for the classification of R71 as a less luminous LBV comes from the fact that its visual light and temperature variation during the 1970s outburst showed much smaller variations than is observed for the more luminous LBVs (Thackeray 1974; Wolf et al. 1981). Further evidence in favor of a RSG phase comes from infrared studies. A dust shell around R71 may have been produced in a short RSG phase (Voors et al. 1999; van Loon et al. 2010; Boyer et al. 2010). If the period-luminosity relation for LBVs found by Stothers & Chin (1995) holds for R71, then the timescale of about 40 years between the current eruption and its 1970s outburst implies $M_{bol} \sim -9$ mag (only 20 years between outbursts would have been expected in case of $M_{bol} \sim -10$ mag).

Lennon et al. (1993), however, argued that the extinction toward R71 is anomalous and greater than previously thought and thus found a much higher luminosity and temperature, more consistent with a spectral type of B2.5 Ieq. R71 enters the region of classical LBVs in the HR diagram, if we adopt the extinction value found by Lennon et al. (1993). Its 1970s outburst may have been unusually weak compared to other classical LBV outbursts.

R71 does not appear to lie in a region with anomalous extinction, see, e.g., Fig. 11 in Imara & Blitz (2007) and Fig. 5 in Dobashi et al. (2008). The empirical relation between sodium absorption and dust extinction found by Poznanski et al. (2012) and $R_V = 3.1$ implies an interstellar extinction of $A_V = 0.09 \pm 0.03$ mag toward R71. This value is likely too low. Boyer et al. (2010), e.g., assumed $A_V = 0.4$ mag based on the extinction map by Schlegel et al. (1998). A potential larger extinction toward R71 would likely be of circumstellar nature and may be caused by dust formed in carbon deficient ejecta (Lennon et al. 1993) but interstellar origin cannot be excluded (Voors et al. 1999). An upper limit to the extinction toward R71 of $A_{V,2012} < 0.7 \pm 0.4$ mag can be inferred from the absence of the λ10780 absorption line for which a relation between the line equivalent width and $E(B-V)$ was found by Groh et al. (2007). While this upper limit does not discriminate against any of the extinction values found in the literature, it implies that the current extinction value is certainly not much higher than the pre-eruption value. The use of other diffuse interstellar medium lines and their correlation with extinction is inhibited because line identification is made impossible by many small emission and absorption lines even in R71's quiescent state. R71 has likely an extinction value of $0.1 < A_V < 1.1$ mag and thus lies close to the boundary between the less luminous and the classical LBVs during its quiescent state and a previous short RSG phase cannot entirely be ruled out.

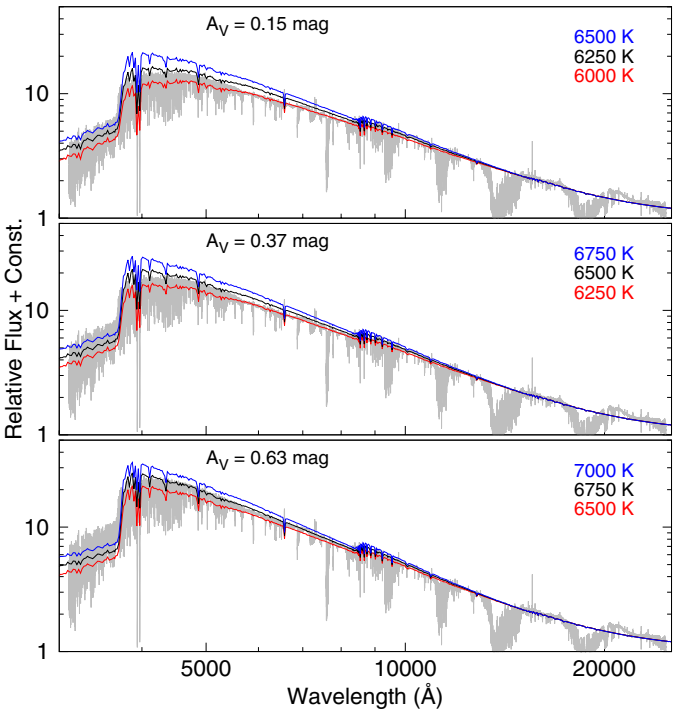

Fig. 5. Comparison of de-reddened X-shooter spectra from 2012 November and Kurucz model atmospheres ([Fe/H] = −0.5, log g = 0.5). Both axes are scaled logarithmically. The continuum energy distribution is well fitted for the extinction values A_V found in the literature. Higher extinction values require models with slightly higher effective temperatures.

The observed spectral changes during R71's current eruption are expected in an outburst that produces an optically thick wind (Humphreys & Davidson 1994) but it is not well-established if LBVs do form pseudo-photospheres. Leitherer et al. (1989)

and de Koter et al. (1996) found based on NLTE modeling that the observed variability of the photospheric radius and effective temperature cannot be due to the formation of a pseudo-photosphere but must be induced by a subphotospheric instability and an actual increase of the radius of the stellar core. Smith et al. (2004), on the other hand, argued that objects close to the bi-stability jump and close to the Eddington limit could form pseudo-photospheres. In our discussion we adopt the pseudo-photosphere hypothesis, i.e., that the apparent changes in R71's spectrum and photometry are caused in the outermost layers. However, we are aware that the discussion is still open on this issue.

Estimations of R71's current effective temperature based on intrinsic colors are likely to fail because LBVs and R71 in particular show generally a UV excess (Wolf et al. 1980; Lennon et al. 1993) and the reddening toward R71 is disputed. For example, the relation between $T_{\rm eff}$ and $(B-V)_0$ found by Neugent et al. (2010) results in $T_{\rm eff}$ = 5600–6000 K if we adopt $(B-V)$ = 0.6 mag (AAVSO) and allow for different extinction values. However, spectral features and the X-shooter spectral energy distribution imply a higher effective temperature. To determine R71's apparent temperature we used the line-depth ratios described in Kovtyukh & Gorlova (2000). We determined a current effective temperature of $T_{\rm eff} = 6700 \pm 400$ K. This corresponds to an apparent spectral type of F5 to F8 and a bolometric correction of BC = 0.08–0.13 mag (Humphreys & McElroy 1984). However, the used lines are very weak and mis-identification may have occurred due to the large number of absorption lines in R71's current spectrum.

We also compared the 2012 X-shooter spectra to Kurucz model atmospheres (Castelli et al. 1997). We varied the metallicity from [Fe/H] = 0 to [Fe/H] = −0.5 (close to the literature value $[{\rm Fe/H}]_{\rm LMC} = -0.34$, see Luck et al. 1998), the effective surface gravity $\log g_{\rm eff} = 0.0$ to $\log g_{\rm eff} = 2.0$, and the extinction $A_{\rm V} = 0.15$ to $A_{\rm V} = 0.63$ mag. Two immediate problems arise when comparing the X-shooter spectra to model atmospheres. First, LBVs have weaker Balmer jumps than normal stars. Guo et al. (2005) suggested that this may be due to a decrease of neutral hydrogen because of collisions in the dense wind, due to extra emission from the recombination of hydrogen, or due to the more extended atmospheres in which the velocity field changes with the radius and the lines of the Lyman series could be spread out. Guo & Li (2007) showed that the continuum energy distribution around the Balmer jump is sensitive to the wind velocity law. Second, the observed spectral energy distribution of LBVs in outburst may be a combination of two sources (the central star and the envelope). Guo et al. (2005) proposed that LBVs form a nonhomogeneous envelope during outburst, which is not optically thick in all directions. The observed spectral energy distribution comes from the central star (mostly in the UV) as well as the optically thick part of the envelope (mostly in the optical wavelength regions). When comparing model atmospheres to the X-shooter spectra we thus focus on the continuum emission redwards of the Balmer jump.

Models with higher surface gravity $\log g$ have weaker Balmer and Paschen jumps. Because of the above described issues, we make an apriori assumption about $\log g$. Lennon et al. (1993) found $\log g = 1.8$ for R71 in quiescent state. The effective surface gravity in 2012 is likely $\log g_{\rm eff,2012} \lesssim 0.5$ based on the fact that R71's effective radius has increased by up to a factor of 5, see below, and that low effective gravities of $\log g_{\rm eff} = 0.5$–1.0 were found for several LBVs in outburst. For example, Sterken et al. (1991) estimated $\log g_{\rm eff} = 0.55$ for HD 160529 and Szeifert et al. (1993) found $\log g_{\rm eff} = 0.75$ for R40. Both objects are similar to R71. Guo et al. (2005) determined $\log g_{\rm eff} = 1$ for R127 and $\log g_{\rm eff} = 0.5$ for R110. We thus adopt $\log g_{\rm eff,2012} = 0.5$ for R71, also on the grounds that for lower surface gravities the models become unstable against radiation pressure.

Figure 5 shows de-reddened ($A_{\rm V} = 0.15, 0.37, 0.63$ mag) 2012 November X-shooter spectra and model atmospheres of different effective temperatures. The analytic formula for the mean extinction law by Cardelli et al. (1989) and $R_{\rm V} = 3.1$ (Howarth 1983) were adopted to de-redden the X-shooter spectra. In each case the best fit leads to a too high Balmer discontinuity, but see above. Unfortunately, we cannot discriminate between the different values of $A_{\rm V}$ used in the literature. For higher extinction values the X-shooter spectra are well fitted by model atmospheres with higher effective temperatures. We find that model atmospheres with $T_{\rm eff} = 6600 \pm 300$ K fit best the spectral energy distribution of our X-shooter spectra, if we take the range of extinction values $A_{\rm V} = 0.15$–0.63 mag into account. The derived effective temperature from model atmospheres is very similar to the value from the line ratio measurements discussed above. R71's pseudo-photosphere has certainly reached much lower temperatures than during its 1970s outburst when the apparent temperature was not cooler than $T_{\rm eff} \sim 8\,150$ K. However, we do not confirm the result by Gamen et al. (2012) that R71 has currently an early G-supergiant spectrum and thus a temperature below 6000 K (Humphreys & McElroy 1984).

While there is uncertainty of R71's parameters during its quiescent state because of uncertainties in the extinction $A_{\rm V}$ and the bolometric correction BC (see Table 2 and above discussion), its current temperature implies a low value for BC. We adopt a distance modulus of $DM_{\rm LMC} = 18.5$ mag (e.g., Freedman et al. 2001; Pietrzyński et al. 2013), a visual extinction of $A_{\rm V} = 0.15$–0.63 mag, and a bolometric correction of $BC = 0.11$ mag, and find that R71's current visual brightness of $m_{\rm V,2012} = 8.7$ mag results in $M_{\rm bol,2012} \sim -9.8$ mag to -10.3 mag. R71's luminosity of $\log L_{\rm R71,2012}/L_\odot = 5.8$–$6.0$ is about its classical Eddington luminosity ($\log L_{\rm R71,Edd}/L_\odot \sim 5.8$–$6.1$). The pre-eruption bolometric luminosity was $M_{\rm bol,quiescence} \sim -8.5$ mag to -9.9 mag if we adopt $DM_{\rm LMC} = 18.5$ mag instead of the varying distance moduli used in the literature[6]. The bolometric luminosity thus increased by 0.4–1.3 mag.

The very low effective temperature of R71's pseudo-photosphere during the current eruption below 7500 K implies a very high wind density (Davidson 1987). LBVs in quiescence have mass loss rates comparable to normal supergiants of the same temperature and luminosity (10^{-7} $M_\odot$ yr^{-1} to 10^{-5} $M_\odot$ yr^{-1}), which increase 10–100 times during an outburst. R71's mass loss rate during its quiescent state was 3×10^{-7} $M_\odot$ yr^{-1} and during its 1970s outburst 5×10^{-5} $M_\odot$ yr^{-1} (Wolf et al. 1981). Davidson (1987) estimated the apparent temperature of LBV outbursts as a function of mass loss rate and luminosity using a simple radiative transfer model of an opaque wind. We use Fig. 1 and Eq. (4) of Davidson (1987) for a rough estimate of R71's current mass loss rate and find $\dot{M}_{\rm R71,2012} \sim 7 \times 10^{-5}$ $M_\odot$ yr^{-1} to 7×10^{-3} $M_\odot$ yr^{-1}. We also follow the argument by Wolf et al. (1980), who derived the mass loss rate of S Dor using the formula $\dot{M} = 4\pi R^2 \mu n_{\rm H} m_{\rm H} v_{\rm exp}$. We assume similar physical conditions but substitute R and $v_{\rm exp}$ for the values found for R71 ($R = 500\,R_\odot$, $v_{\rm exp} = 10$ km s^{-1}) and find a current mass loss rate of $\dot{M}_{\rm R71,2012} \sim 2 \times 10^{-4}$ $M_\odot$ yr^{-1}. Both methods are only order of magnitude estimates. The determination of

[6] The range of the pre-eruption bolometric luminosity is larger because of the greater uncertainty in the bolometric correction BC.

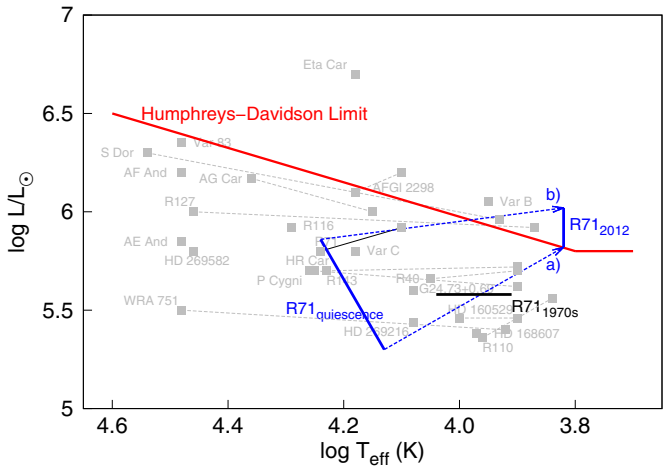

Fig. 6. Schematic upper HR diagram. The red solid curve is the upper luminosity boundary. Confirmed LBVs (in the Galaxy, LMC, SMC, M31, and M33) and their transitions during outburst are displayed in gray. Values for L and T are retrieved mostly from van Genderen (2001), but for AG Car (Groh et al. 2009b), HR Car (Groh et al. 2009a), AFGl 2298 (Clark et al. 2003), G24.73+0.69 (Clark et al. 2005), WRA 751 (Sterken et al. 2008), and the M31 and M33 LBVs AE And, AF And, Var B, Var C, Var 83 (Szeifert et al. 1996). The positions of R71 during its quiescent state and its current eruption are indicated with blue solid curves. The lines do not imply variability but the range of loci permitted by the uncertainty of the reddening data and the bolometric correction. The dashed blue curves show the transitions for the lowest and highest extinction values found in the literature; (a) $A_V = 0.15$ mag and (b) $A_V = 0.63$ mag. R71's 1970s outburst location is indicated in black.

stellar parameters such as mass loss rate by quantitative radiative transfer codes is beyond the scope of this paper. Radiative transfer codes like CMFGEN (Hillier & Lanz 2001) are designed for LBV atmospheres and winds but are not applicable for temperatures below 7000 K.

R71 increased its mass loss rate by a factor of about 1000. The total mass of ejected material during the last 6 years may therefore be on the order of 10^{-3} $M_\odot$. We find no evidence of an explosion. The spectra show no signatures of fast moving material and the terminal velocity is comparable to R71's quiescent state. Also, during its 1970s outburst the terminal velocity was similar (Wolf et al. 1981). This indicates that the change in mass loss rate is caused by a tremendously increased wind density only. The effective radius increased by a factor of about 5 from 81–95 $R_\odot$ (Wolf et al. 1981; Lennon et al. 1993) during the quiescent phase and is now on the order of 500 $R_\odot$. This radius estimation is based on the apparent temperature and luminosity during the eruption and may not be very meaningful because the opacity in the pseudo-photosphere is mainly due to scattering (Davidson 1987).

Figure 6 shows the location of R71 in quiescence and during its current eruptive state in the HR diagram. The solid blue lines indicate the range of bolometric luminosities obtained for each state if we adopt $DM_{LMC} = 18.5$ mag and the different values for A_V and BC found in the literature, see Table 2. The dashed blue lines indicate the transitions for the two extreme cases. The transition labeled "(a)" is the transition for the lowest extinction value, $A_V = 0.15$ mag, and the transition labeled "(b)" is the transition for the highest extinction value $A_V = 0.63$ mag. R71 could have potentially increased its bolometric luminosity by up to 1.3 mag. The black curve shows the location of R71 in the HR diagram during its 1970s outburst, which is quite different.

R71's visual magnitude variation on the order of $\Delta m_V \sim 2$ mag implies that the star is experiencing a classical LBV outburst (Humphreys & Davidson 1994). However, the effective temperature appears to be unusually low and the mass loss rate unusually high. Also, the common (but possibly false, see Fig. 6) notion is that during classical LBV outbursts the bolometric luminosity stays constant, which is most likely not the case for R71's current eruption. With a growing number of observed LBV outbursts and with the realization that outbursts of the same object can differ considerably this commonly adopted classification scheme may have to be reconsidered.

5. Conclusion

R71's current eruption differs from its 1970s classical LBV outburst in several aspects and is challenging our view on LBVs. Both the visual lightcurve and the spectra show many differences compared to its previous outburst. The visual light increased by $\Delta m_V \gtrsim 2$ mag over the last seven years and the spectrum indicates an unusually low temperature of R71's pseudo-photosphere, mimicking the photosphere of a late-F supergiant. Balmer and Fe II P Cyg profiles, normally observed during LBV outbursts and present during R71's previous 1970s outburst, are absent. Low-excitation forbidden emission lines and Fe I P Cyg-like profiles appear in late 2012.

We found an apparent temperature of R71 in 2012 of $T_{eff,2012} \sim 6650$ K. This is a decrease by more than 7000 K compared to its quiescent state and more than 1500 K cooler than during its 1970s outburst. The bolometric luminosity increased by 0.4–1.3 mag to $M_{bol,2012} \sim -9.8$ mag to -10.3 mag and R71 may have moved beyond the Humphreys-Davidson limit. R71's apparent radius increased by a factor of 5 to about 500 $R_\odot$.

We estimated that R71 has a current mass loss rate on the order of $\dot{M}_{R71,2012} \sim 5 \times 10^{-4}$ $M_\odot$ yr^{-1}, a factor of about 1000 higher than during its quiescent state and at least a factor of 10 larger than during its 1970s outburst. The wind velocity of R71 is on the order of 100–200 km s^{-1}, similar to that of other LBVs while the pseudo-photosphere has a velocity on the order of a few km s^{-1}. We find no spectral signatures of fast moving material, which may indicate an explosion. The large increase in mass loss rate during the eruption is therefore likely due to an increased wind density only, thus constraining instability mechanisms.

Wolf (1989) found a relation between the luminosity of LBVs and their outburst amplitudes. However, with an increasing number of observed LBV outbursts it becomes clear that they can differ considerably – even outbursts of the same object. S Dor, e.g., displayed an early F-type supergiant spectrum in 1999, which had never been reported before, while its visual luminosity only increased by 0.3 mag (Massey 2000). The current eruption of R71 has a much larger amplitude than its previous outburst in the 1970s[7].

R71 is experiencing a much more powerful LBV eruption than during its 1970s outburst. We are in the unique position to witness such a rare event as it unfolds. Our X-shooter monitoring program on R71 will secure key data for our understanding of LBV outbursts and the properties of stars near the upper luminosity limit. Observations in the infrared after the eruption has

[7] LBVs have been considered as extragalactic distance indicators because they belong to the most luminous stars (e.g., Tammann & Sandage 1968; Sandage 1983, 1984). However, the variations observed between different LBV outbursts of the same object demonstrate that they are unreliable as distance indicators.

subsided are highly desirable because they will provide valuable information about the total amount of material expelled.

Acknowledgements. We thank the Paranal Observatory for conducting the observations and ESO for the acceptance of our DDT program. We acknowledge with thanks the variable star observations from the AAVSO International Database contributed by observers worldwide and used in this research. We also thank Roberta M. Humphreys, Willem-Jan de Wit, Jose Groh, and Noel Richardson for valuable discussions.

References

Appenzeller, I. 1986, in Luminous Stars and Associations in Galaxies, eds. C. W. H. De Loore, A. J. Willis, & P. Laskarides, IAU Symp., 116, 139
Boyer, M. L., Sargent, B., van Loon, J. T., et al. 2010, A&A, 518, L142
Cardelli, J. A., Clayton, G. C., & Mathis, J. S. 1989, ApJ, 345, 245
Castelli, F., Gratton, R. G., & Kurucz, R. L. 1997, A&A, 318, 841
Clark, J. S., Larionov, V. M., Crowther, P. A., Egan, M. P., & Arkharov, A. 2003, A&A, 403, 653
Clark, J. S., Larionov, V. M., & Arkharov, A. 2005, A&A, 435, 239
Conti, P. S. 1984, in Observational Tests of the Stellar Evolution Theory, eds. A. Maeder, & A. Renzini, IAU Symp., 105, 233
Conti, P. S. 1997, in Luminous Blue Variables: Massive Stars in Transition, eds. A. Nota, & H. Lamers, PASPC, 120, 387
Davidson, K. 1987, ApJ, 317, 760
Davidson, K., & Humphreys, R. M. 1997, ARA&A, 35, 1
Davidson, K., & Humphreys, R. M. 2012, Eta Carinae and the Supernova Impostors, Astrophysics and Space Science Library, 384
de Groot, M. 1988, Ir. Astron. J., 18, 163
de Koter, A., Lamers, H. J. G. L. M., & Schmutz, W. 1996, A&A, 306, 501
Dobashi, K., Bernard, J.-P., Hughes, A., et al. 2008, A&A, 484, 205
Feast, M. W., Thackeray, A. D., & Wesselink, A. J. 1960, MNRAS, 121, 337
Freedman, W. L., Madore, B. F., Gibson, B. K., et al. 2001, ApJ, 553, 47
Gal-Yam, A., & Leonard, D. C. 2009, Nature, 458, 865
Gal-Yam, A., Leonard, D. C., Fox, D. B., et al. 2007, ApJ, 656, 372
Gamen, R., Barba, R., Walborn, N., et al. 2009, IAU Circ., 9082, 1
Gamen, R., Walborn, N., Morrell, N., Barba, R., & Fernandez Lajus, E. 2012, Central Bureau Electronic Telegrams, 3192, 1
Goodrich, R. W., Stringfellow, G. S., Penrod, G. D., & Filippenko, A. V. 1989, ApJ, 342, 908
Groh, J. H., Damineli, A., & Jablonski, F. 2007, A&A, 465, 993
Groh, J. H., Damineli, A., Hillier, D. J., et al. 2009a, ApJ, 705, L25
Groh, J. H., Hillier, D. J., Damineli, A., et al. 2009b, ApJ, 698, 1698
Groh, J. H., Meynet, G., & Ekström, S. 2013, A&A, 550, L7
Guo, J. H., & Li, Y. 2007, ApJ, 659, 1563
Guo, J.-H., Li, Y., & Shan, H.-G. 2005, Chinese J. Astron. Astrophys., 5, 245
Hillier, D. J., & Lanz, T. 2001, in Spectroscopic Challenges of Photoionized Plasmas, eds. G. Ferland, & D. W. Savin, ASP Conf. Ser., 247, 343
Howarth, I. D. 1983, MNRAS, 203, 301
Humphreys, R. M., & Davidson, K. 1979, ApJ, 232, 409
Humphreys, R. M., & Davidson, K. 1984, Science, 223, 243
Humphreys, R. M., & Davidson, K. 1994, PASP, 106, 1025
Humphreys, R. M., & McElroy, D. B. 1984, ApJ, 284, 565
Imara, N., & Blitz, L. 2007, ApJ, 662, 969
Kochanek, C. S., Szczygiel, D. M., & Stanek, K. Z. 2011, ApJ, 737, 76
Kovtyukh, V. V., & Gorlova, N. I. 2000, A&A, 358, 587
Kovtyukh, V. V., Wallerstein, G., Andrievsky, S. M., et al. 2011, A&A, 526, A116
Lamers, H. J. G. L. M., & de Groot, M. J. H. 1992, A&A, 257, 153
Lamers, H. J. G. L. M., Bastiaanse, M. V., Aerts, C., & Spoon, H. W. W. 1998, A&A, 335, 605
Langer, N., Hamann, W.-R., Lennon, M., et al. 1994, A&A, 290, 819
Leitherer, C., Appenzeller, I., Klare, G., et al. 1985, A&A, 153, 168
Leitherer, C., Schmutz, W., Abbott, D. C., Hamann, W.-R., & Wessolowski, U. 1989, ApJ, 346, 919
Lennon, D. J., Wobig, D., Kudritzki, R.-P., & Stahl, O. 1993, Space Sci. Rev., 66, 207
Luck, R. E., Moffett, T. J., Barnes, III, T. G., & Gieren, W. P. 1998, AJ, 115, 605
Maeder, A. 1983, A&A, 120, 113
Massey, P. 2000, PASP, 112, 144
Neugent, K. F., Massey, P., Skiff, B., et al. 2010, ApJ, 719, 1784
Nota, A., & Lamers, H. 1997, Luminous Blue Variables: Massive Stars in Transition, ASPC, 120
Pietrzyński, G., Graczyk, D., Gieren, W., et al. 2013, Nature, 495, 76
Pojmanski, G. 1997, Acta Astron., 47, 467
Poznanski, D., Prochaska, J. X., & Bloom, J. S. 2012, MNRAS, 426, 1465
Prieto, J. L., Sellgren, K., Thompson, T. A., & Kochanek, C. S. 2009, ApJ, 705, 1425
Quataert, E., & Shiode, J. 2012, MNRAS, 423, L92
Sandage, A. 1983, AJ, 88, 1569
Sandage, A. 1984, AJ, 89, 630
Schlegel, D. J., Finkbeiner, D. P., & Davis, M. 1998, ApJ, 500, 525
Smith, N., Humphreys, R. M., & Gehrz, R. D. 2001, PASP, 113, 692
Smith, N., Vink, J. S., & de Koter, A. 2004, ApJ, 615, 475
Smith, N., Li, W., Foley, R. J., et al. 2007, ApJ, 666, 1116
Smith, N., Chornock, R., Li, W., et al. 2008, ApJ, 686, 467
Smith, N., Ganeshalingam, M., Chornock, R., et al. 2009, ApJ, 697, L49
Stahl, O., & Wolf, B. 1986, A&A, 158, 371
Sterken, C., Gosset, E., Juttner, A., et al. 1991, A&A, 247, 383
Sterken, C., van Genderen, A. M., Plummer, A., & Jones, A. F. 2008, A&A, 484, 463
Stothers, R. B., & Chin, C.-W. 1995, ApJ, 451, L61
Szeifert, T., Stahl, O., Wolf, B., et al. 1993, A&A, 280, 508
Szeifert, T., Humphreys, R. M., Davidson, K., et al. 1996, A&A, 314, 131
Tammann, G. A., & Sandage, A. 1968, ApJ, 151, 825
Thackeray, A. D. 1974, MNRAS, 168, 221
Van Dyk, S. D., & Matheson, T. 2012, ApJ, 746, 179
van Genderen, A. M. 1979, A&AS, 38, 151
van Genderen, A. M. 1982, A&A, 112, 61
van Genderen, A. M. 2001, A&A, 366, 508
van Genderen, A. M., Steemers, W. J. G., Feldbrugge, P. T. M., et al. 1985, A&A, 153, 163
van Genderen, A. M., The, P. S., Augusteijn, T., et al. 1988, A&AS, 74, 453
van Genderen, A. M., de Groot, M., & Sterken, C. 1997, A&AS, 124, 517
van Loon, J. T., Oliveira, J. M., Gordon, K. D., et al. 2010, AJ, 139, 68
Vernet, J., Dekker, H., D'Odorico, S., et al. 2011, A&A, 536, A105
Vink, J. S., & de Koter, A. 2002, A&A, 393, 543
Voors, R. H. M., Waters, L. B. F. M., Morris, P. W., et al. 1999, A&A, 341, L67
Weis, K. 2003, A&A, 408, 205
Wolf, B. 1975, A&A, 41, 471
Wolf, B. 1989, A&A, 217, 87
Wolf, B., Appenzeller, I., & Cassatella, A. 1980, A&A, 88, 15
Wolf, B., Appenzeller, I., & Stahl, O. 1981, A&A, 103, 94

Table 1. Journal of observations.

Date	MJD (days)	Instrument	Wavelength range (Å)	Spectral resolving power	Total exposure time (s)
2002-07-23	52 478.4	UVES	3260–4450	40 000	360
2002-07-23	52 478.4	UVES	4580–6680	40 000	3×110
2002-08-03	52 489.4	UVES	3260–4450	40 000	360
2002-08-03	52 489.4	UVES	4580–6680	40 000	3×110
2002-08-12	52 498.4	UVES	3260–4450	40 000	360
2002-08-12	52 498.4	UVES	4580–6680	40 000	3×110
2002-09-04	52 521.4	UVES	3260–4450	40 000	360
2002-09-04	52 521.4	UVES	4580–6680	40 000	3×110
2002-09-10	52 527.4	UVES	3260–4450	40 000	360
2002-09-10	52 527.4	UVES	4580–6680	40 000	3×110
2002-09-18	52 535.3	UVES	3260–4450	40 000	360
2002-09-18	52535.3	UVES	4580–6680	40 000	3×110
2002-09-22	52 539.3	UVES	3260–4450	40 000	360
2002-09-22	52 539.3	UVES	4580–6680	40 000	3×110
2002-09-30	52 547.4	UVES	3260–4450	40 000	360
2002-09-30	52 547.4	UVES	4580–6680	40 000	3×110
2002-10-06	52 553.4	UVES	3260–4450	40 000	360
2002-10-06	52 553.4	UVES	4580–6680	40 000	3×110
2005-12-12	53 716.2	FEROS	3500–9200	48 000	2×450
2007-02-22	54 153.2	FEROS	3500–9200	48 000	3×500
2011-03-20	55 641.0	FEROS	3500–9200	48 000	1800
2011-05-15	55 697.0	FEROS	3500–9200	48 000	1800
2012-08-26	56 165.3	X-shooter	10 240–24 800	10 000	3×60^{1}, 2×10^{2}
2012-08-26	56 165.3	X-shooter	3000–5595	9000	3×120^{1}, 2×20^{2}
2012-08-26	56 165.3	X-shooter	5595–10 240	17 000	3×120^{1}, 2×20^{2}
2012-09-04	56 174.3	X-shooter	10 240–24 800	10 000	3×60^{1}, 2×10^{2}
2012-09-04	56 174.3	X-shooter	3000–5595	9000	3×120^{1}, 2×20^{2}
2012-09-04	56 174.3	X-shooter	5595–10 240	17 000	3×120^{1}, 2×20^{2}
2012-11-01	56 232.2	X-shooter	10 240–24 800	10 000	3×60^{1}, 2×10^{2}
2012-11-01	56 232.2	X-shooter	3000–5595	9000	3×120^{1}, 2×20^{2}
2012-11-01	56 232.2	X-shooter	5595–10 240	17 000	3×120^{1}, 2×20^{2}

Notes. [(1)] Slit width: 0.″5/0.″4/0.″4 for the UVB/VIS/NIR arms. [(2)] Slit width: 5″/5″/5″ for the UVB/VIS/NIR arms.